ARMA 15-0028

SAND2015-1488C

Behavior of salt from the Bayou Choctaw salt dome

Ingraham, M.D., Broome, S.T., Bauer, S.J., Barrow, P.C. and Flint, G.M.

Sandia National Laboratory, Albuquerque, NM, USA

This paper was prepared for presentation at the 49th US Rock Mechanics / Geomechanics Symposium held in San Francisco, CA, USA, 28 June-1 July 2015.

ABSTRACT: A laboratory testing program was developed to examine the short-term mechanical and time-dependent (creep) behavior of salt from the Bayou Choctaw Salt Dome. Core was tested under creep and quasi-static constant mean stress axisymmetric compression, and constant mean stress axisymmetric extension conditions. Creep tests were performed at 38 degrees Celsius, and the axisymmetric tests were performed at ambient temperatures (22-26 degrees Celsius). The testing performed indicates that the dilation criterion is pressure and stress state dependent. It was found that as the mean stress increases, the shear stress required to cause dilation increases. The results for this salt are reasonably consistent with those observed for other domal salts. Also it was observed that tests performed under extensile conditions required consistently lower shear stress to cause dilation for the same mean stress, which is consistent with other domal salts. Young's modulus ranged from 27.2 to 58.7 GPa with an average of 44.4 GPa, with Poisson's ratio ranging from 0.10 to 0.43 with an average of 0.30. Creep testing indicates that the BC salt is intermediate in creep resistance when compared with other bedded and domal salt steady-state behavior.

1. INTRODUCTION

Sandia National Laboratories, on behalf of The U.S. Department of Energy (DOE), is evaluating the mechanical integrity of the salt pillars surrounding existing petroleum storage caverns in the Bayou Choctaw Dome (Louisiana) that are part of the U.S. Strategic Petroleum Reserve (SPR). The purpose of this experimental effort is to better characterize the salt strength, dilational strength and creep in the salt section above Cavern 102 and below the overlying abandoned caverns, where casing issues have been observed [1].

The core used for this experimental study was obtained from a drill hole from depths of 325 to 335 meters below ground surface (bgs) and is above one of the Bayou Choctaw SPR caverns. For reference the top of the salt dome lies between 183 and 213 meters bgs, and the total depth is over 3050 meters bgs. The natural rock salt deposits used in the SPR are ideal for storage of crude oil because of their low (nearly zero) permeability, ease of mining, and proximity to shipping and refining operations.

The mechanical behavior of rock salt is relatively unique when compared with other geologic media due to the well-known ability of salt to show significant time dependent deformation without fracturing when subjected to differential stresses [2]. This can result in the closure of caverns and mines over time, which results in reduced storage in the case of caverns. Under some differential stress states salt is known to dilate due to stress-induced microfracturing [3].

In this work elastic properties and dilation behavior were determined by performing constant mean stress axisymmetric compression (ASC) and axisymmetric extension (ASE) tests. Creep properties were determined using standard constant differential stress creep tests. While the composition of the salt used in this testing was not quantitatively determined, it was determined, from visual observation, that the salt is relatively pure halite with impurities comprising less than 2-4% by volume. Impurities appeared to be anhydrite.

2. SPECIMEN PREPARATION

Specimens used for axisymmetric compression and creep testing were nominally 101.6 mm in diameter and 203.2 mm long. These were made using the as-received core diameter. Specimens used for the axisymmetric extension tests were 69.9 mm in diameter and 139.7 mm in length. This specimen size was required to perform the extension tests as the piston of the vessel used for testing was 76.2 mm in diameter and for extension testing the specimen diameter must be smaller than the piston diameter to achieve the necessary stress state.

Specimens were first cut to an approximate length using a wire saw or band saw (depending on proximity to the end of the core). The smaller specimens were then

subcored to 76.2 mm in diameter and ground on a lathe to the final diameter of 69.9 mm to ensure roundness. After grinding and sawing, the specimens were ground on a surface grinder using a sanding wheel. This was done to ensure the ends were parallel to one another and perpendicular to the core axis. These were ground with a parallelism tolerance of .0254 mm per mm of specimen diameter per ASTM standard D-4543 [4].

Imperfections in the surface of the specimens (e.g. plucked grains) were filled with Ultracal® plaster. Specimens were then stored in a 50°C oven for at least 48 hours prior to jacketing. The imperfections were filled to ensure that confining jackets would not rupture due to a void in the specimen when pressurized. Specimen depth, specimen properties, and testing type are summarized in Table 1.

During jacketing the end surfaces of the specimens were lubricated using a stearic acid and petroleum jelly lubricant [5]. A 12.7 mm ring of viton was then placed around the specimen-end cap interface at the top and bottom of the specimen to bridge any gaps between the pieces and mitigate the likelihood of a jacket leak. Axisymmetric tests were jacketed with an o-ring on each end cap surrounded by a polyvinyl chloride (heat shrink) tubing and secured on either side of each o-ring with tie wire. The jackets of the creep tests were similar save that a viton jacket was used; the o-ring and tie wire seal was the same for these tests.

Table 1. Specimen ID, depth, density and test type

Test #	Depth bgs (m)	Density (g/cc)	Test Type
1	326.2	2.151	Creep
2	326.0	2.163	ASC
3	325.8	2.160	ASE
4	328.8	2.149	Creep
5	328.5	2.158	ASC
6	328.4	2.162	ASE
7	329.2	2.152	Creep
8	329.4	2.154	ASC
9	329.6	2.160	ASE
10	330.1	2.158	Creep
11	330.3	2.155	ASC
12	330.5	2.155	ASE
13	331.9	2.153	Creep
14	332.1	2.155	ASC
15	332.5	2.159	ASE
16	333.0	2.141	Creep
17	333.2	2.154	ASC
18	333.4	2.147	ASE
19	334.0	2.153	Creep
20	334.2	2.163	ASC
21	334.5	2.156	ASE

For the axisymmetric tests, both extension and compression specimens were instrumented with linear variable displacement transformers (LVDTs) to measure displacement in the axial and radial directions. An image of an instrumented and jacketed specimen is shown in Figure 1.

Deformations for the creep tests were measured by transducers mounted inside and outside the pressure vessel. Axial deformation was measured by a pair of internal LVDTs as well as two external LVDTs within their linear range (2.54 mm and 25.4 mm) that tracked the displacement of the axial push-rod relative to the bottom of the pressure vessel. This displacement was a direct measure of the axial displacement of the specimen because non-specimen deformations were negligible given the imposed constant stress condition. The external LVDTs were mounted 180º apart on the push-rod. During the tests, the 2.54-mm-range LVDTs were reset periodically when the range was exceeded. Radial displacements were measured directly with a Schueler gage mounted on the specimen.

Prior to testing all of the axisymmetric tests were conditioned isostatically at 34.5 MPa for at least 12 hours at room temperature to help ensure that any cracks or grain boundaries were pushed together to create a test more consistent and representative of the condition of the salt at depth. For creep tests specimens were conditioned at7.6 MPa and 38 degrees C (test conditions) for at least 12 hours.

Fig. 1. Instrumented and jacketed specimen, this is axisymmetric compression specimen #11 post-test.

3. TEST PROCEDURE

3.1. Axisymmetric Tests

Both axisymmetric compression and axisymmetric extension tests were performed under constant mean stress conditions. This means that once the desired mean stress was reached hydrostatically, the control mode of the test frame was changed to maintain the mean stress. This is achieved under axisymmetric compression conditions by increasing the axial load in displacement control (approximating $5x10^{-5}$ sec^{-1} strain rate), while a calculated control channel decreased the confining pressure by the required amount to maintain constant mean stress on the specimen as the axial stress increased. For a system such as this where the intermediate and minimum principal stresses are applied by confining fluid and therefore equal, for every increment the axial stress increases (maximum principal stress, parallel to the central axis), the confining pressure decreases by half of the increment of axial stress.

After instrumentation, the specimens were loaded into the vessel and conditioned overnight. After the specimens were conditioned, hydrostatic pressure was lowered from the conditioning pressure to the desired constant mean stress. Then an unload-reload cycle was performed at constant confining pressure to determine Young's modulus for the specimen at test pressure. Then the constant mean stress control was initiated and the specimen was loaded under constant mean stress conditions. Unload-reload cycles were performed under the constant mean stress condition at the discretion of the testing personnel during loading. Tests were run until the specimen was determined to have dilated (monitored through a calculated volume strain channel in the control system) or until the specimen jacket leaked. Unloading was the reverse of loading, the specimen was returned to a hydrostatic state of stress, which was then decreased to atmospheric pressure.

Axisymmetric extension testing was largely the same as the axisymmetric compression testing, with a few small changes. First the specimens were smaller to allow a sealing ring to be placed between the specimen and the baseplate in the pressure vessel as well as between the specimen and the piston. This allowed isolation of the confining pressure from contacting the end of the specimen allowing the axial stress to be unloaded from the specimen below the confining pressure, thereby conducting an extension test. To ensure the sealing ring maintained a seal between the sample and the vessel/piston an axial stress of 2 MPa over hydrostatic was maintained on the specimen during hydrostatic loading.

Then the axial stress was decreased in displacement control (approximately $1.5x10^{-5}$ sec^{-1} strain rate) while the confining pressure was increased to maintain the constant mean stress condition. As with the compression tests the goal of the test was to determine the onset of dilation therefore, the definition of failure and the end of the test were the same as with the axisymmetric compression tests. As with the axisymmetric compression tests unload-reload loops were performed to monitor the evolution of elastic parameters during testing.

3.2. Creep Tests

The time dependent behavior of the salt was determined through a series of triaxial compression constant stress creep tests. These are similar to the axisymmetric compression tests except that they are performed at a constant axial stress and confining pressure instead of a constant displacement rate with a constant mean stress condition applied. The test is started in the same manner, where hydrostatic pressure is increased to the desired level first (7.6 MPa). The vessel was then heated at constant pressure to 38°C with a set of band heaters clamped around the outside of the vessel and around the loading piston. The temperature was allowed to stabilize for about 24 hours, during which time the specimen was conditioned. After stabilization the axial stress was applied by rapidly increasing the axial load (typically 30-60 seconds to reach target stress). The stress, temperature and confining pressure were maintained constant by an Azonix control system which also recorded data for the creep tests.

Salt specimens undergo rather larger radial expansion during creep testing, as a result the axial force on the specimen needs to change based on the changing specimen diameter. The Azonix system automatically increased the force applied to the specimen based off the long range (25.4 mm) external LVDT reading, assuming constant specimen volume to account for the change in the specimen area. Changing load ensured a constant stress was maintained on the specimen instead of a constant force. Creep tests were ended when the strain rate reached a steady state value or was changing so slowly it could not be discerned. Test durations were typically >50 days.

4. RESULTS AND DISCUSSION

4.1. Axisymmetric Tests

Seven axisymmetric compression tests and seven axisymmetric extension tests were performed on rock salt cores from approximately 325-335 m bgs to determine dilational compressive strengths and static elastic properties. Table 2 summarizes certain key data for the quasistatic testing. This includes the mean stress the test was conducted at, the first invariant of stress at the onset of dilation, I_{1d}, and the Mises equivalent shear stress at the onset of dilation, τ_d. The dilational strength is defined as the shear stress level at the minimum

specimen volume. This is defined as the point at which the volume strain changes from compactant to dilatant, as determined from the stress – strain data collected. This definition is consistent with the literature [6]. Table 2 summarizes the dilational strength results from our laboratory experimental program.

The stress states that produce dilation of pressure-dependent materials are often expressed in terms of two stress invariants, i.e., the first invariant of the Cauchy stress tensor, I_1, and the second invariant of the deviatoric stress tensor, J_2. These two invariants are defined mathematically as:

$$I_1 = \sigma_1 + \sigma_2 + \sigma_3 \quad (1)$$

$$J_2 = \frac{1}{6}\left\{(\sigma_1 - \sigma_2)^2 + (\sigma_2 - \sigma_3)^2 + (\sigma_3 - \sigma_1)^2\right\} \quad (2)$$

where σ_1, σ_2, and σ_3 are the maximum, intermediate, and minimum principal stresses, respectively. For convenience the second invariant number is converted to the Mises equivalent shear which is simply the square root of the second invariant. Note the sign convention used is positive compression, so volume decreases are positive and volume increases are negative.

An example of a typical stress strain curve for an axisymmetric compression test is given in Figure 2. As seen in this figure the stress-strain curve is relatively vertical until about 20 MPa where the specimen behavior changes and begins to compact, until around 45 MPa when the dilation of cracks in the salt overcomes the compaction and the specimen begins to dilate. The large stress drop at approximately 50 MPa is an unload loop to investigate the material properties of the salt at this point during the test.

Figure 3 shows a typical axisymmetric extension test. The initial excursion into the compressive regime, up to about 10 MPa, is from the unload reload cycle performed at constant confining pressure to determine Young's modulus. The rest of the test is in the dilational regime (negative stress). Much like the compression test there is a nearly vertical section of the stress strain curve which ends around 10 MPa, this is much lower than the compression test presented despite the extension test being performed at nearly double the mean stress. The specimen continues to compact until about 30 MPa where dilation takes over and the volume strain direction changes indicating the dilation stress was reached. Note the multiple unload-reload loops performed in this test to monitor the evolution of the shear modulus during testing.

It should be noted that compression test specimens 5, 11, and 14 were wet with confining fluid after testing. This could be due to a jacket leak during the test rendering these strength data unreliable and unusable. Because salt has low permeability it may not be possible to discern a jacket leak during testing. If a leak did occur it would aberrate the mechanical response from the desired conditions. Leaks are suspected in these three specimens and while they are included in data tables they are excluded from analysis used to determine the dilation criteria.

Table 2. Tests performed under axisymmetric compression and axisymmetric extension conditions, showing the mean stress, and values for the first invariant of stress (I_{1d}) and the Mises equivalent shear stress (τ_d) at the dilation limit. *indicates specimen leaked prior to reaching dilation limit.

Test #	Test type	Mean Stress	I_{1d}	τ_d
		(MPa)	(MPa)	(MPa)
2	ASC	10.6	31.7	11.4
3	ASE	29.7	89.1	17.4
5+	ASC	25.0	75.0	4.4
6	ASE	20.7	62.1	12.4
8	ASC	39.1	117.2	28.7
9	ASE	26.2	78.5	*
11+	ASC	27.4	82.1	6.4
12	ASE	35.1	105.4	23.2
14+	ASC	19.8	59.4	6.1
15	ASE	30.8	92.4	8.8
17	ASC	16.2	48.6	25.2
18	ASE	25.6	76.8	17.8
20	ASC	15.3	45.8	15.0
21	ASE	16.1	48.2	*

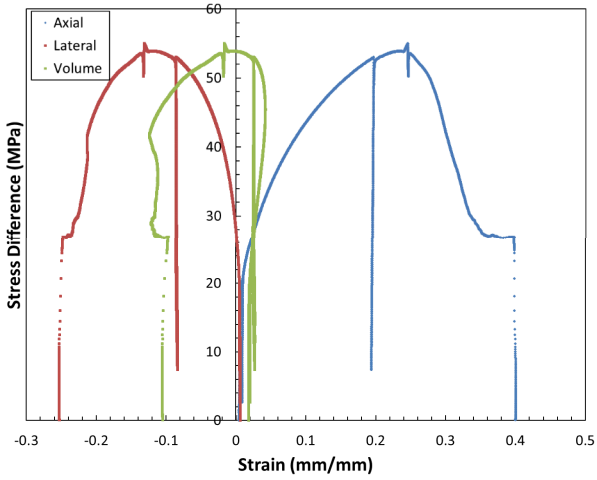

Fig. 2. Stress strain data for a typical axisymmetric compression test, this is test 17 performed at 16.2 MPa mean stress. Differential stress at the onset of dilation was 43.7 MPa which correlates to a Mises equivalent shear stress of 25.2 MPa.

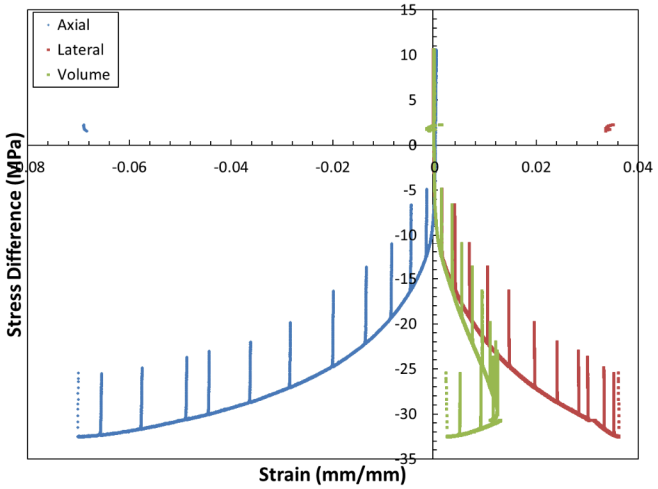

Fig. 3. Stress strain data for a typical axisymmetric extension test, this is test 3, performed at 29.7 MPa. Differential stress at the onset of dilation was 30.1 MPa which correlates to a Mises equivalent shear stress of 17.4 MPa

Leaks also occurred with specimens 9 and 21 (axisymmetric extension). Therefore we include the data in Table 2 but exclude it from analysis of dilation limits. These tests were used for elastic property determinations as data collected prior to leaking is valid. It was known that these specimens leaked because in the extensile stress state a leak caused a sudden pressure drop when fluid came through the pore pressure ports of the vessel indicating that the ends of the specimen were no longer sealed.

Static elastic moduli determined from unload – reload data acquired during the quasi-static constant mean stress compression/extension tests are summarized in Table 3. The static elastic Young's modulus, E_{static}, was determined directly from the slope of the unload/reload stress difference versus axial strain curve. Values of static elastic Poisson's ratio were calculated from the ratio of E_{static} to the slope of the unload/reload stress difference versus lateral strain curve. Young's modulus ranges from approximately 27.2 to 58.7 GPa with an average of 44.4 GPa and generally increased with increasing mean stress. Poisson's ratio ranges from approximately 0.10-0.43 with an average of 0.30.

The experimental dilational strengths are plotted in Figure 4. In Figure 4A, we present the dilatational strength data, plotted in I_1 versus τ space, this line is defined by the equation:

$$\tau = 1932 - 1929e^{-.00008 I_1} \quad (3)$$

for the extension tests, and

$$\tau = 2752 - 2745e^{-.00006 I_1} \quad (4)$$

for the compression tests [7]. These fits are reasonable and make sense for the size of the data set used to generate them. The compression fit is above the extension fit as expected. In Figure 4B the compression fit is compared to existing data sets from the Richton and Big Hill SPR sites as well as the Van Sambeek criteria [7-9].

Table 3. Young's modulus and Poisson's ratio results determined from axisymmetric tests.

Test no.	Young's Modulus,E	Poisson's Ratio
	GPa	
2	30.1	0.10
3	58.7	0.34
6	45.9	0.24
8	53.7	0.30
9	44.0	0.38
12	50.8	0.29
15	45.1	0.33
18	56.0	0.43
20	28.4	0.27
21	48.3	0.37
Average	44.4	0.30

4.2. Creep Tests

A total of seven creep tests were performed. All tests were conducted at a confining pressure of 7.6 MPa, temperature of 38°C, and stress differences ranging from 7.3 to 38.9 MPa (Table 4). The values of temperature and confining pressure were chosen as representative of the in situ conditions of the salt.

Figure 5 plots axial, radial, and volumetric strains versus time and axial strain rate versus time for Test I.D. 13, as an example. The three axial strain curves represent the output from three independent measurements of axial deformation – one using a lower range LVDT (2.54 mm), one using a higher range LVDT (25.4 mm), and one using a pair of internal LVDTs (25.4 mm). Both the axial and radial strain curves are typical of rock salt in that the strain rates are high initially but then decrease monotonically to a constant or nearly constant value over time. In this example, strain rate reaches a constant value (~4.94×10^{-9} s^{-1}) between 50 and 56 days.

Axial strain for each of the seven creep tests is plotted in Figure 6. The respective curves are well ordered in that the smallest strains are seen for the lowest stress difference magnitudes. The experimental value for axial strain rate was calculated from the slope of the axial strain vs. time data. For most tests approximately the last five days of axial strain data were used from each creep test to determine the measured axial (steady-state) strain rate. The highest stress difference test only ran for 4 days and the axial strain rate was determined from the last few hours of test data representing a similar time fraction for this test, as compared with the longer tests.

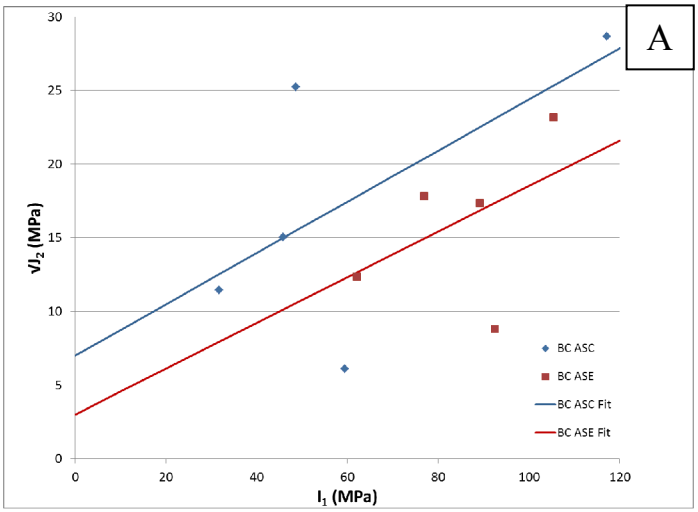

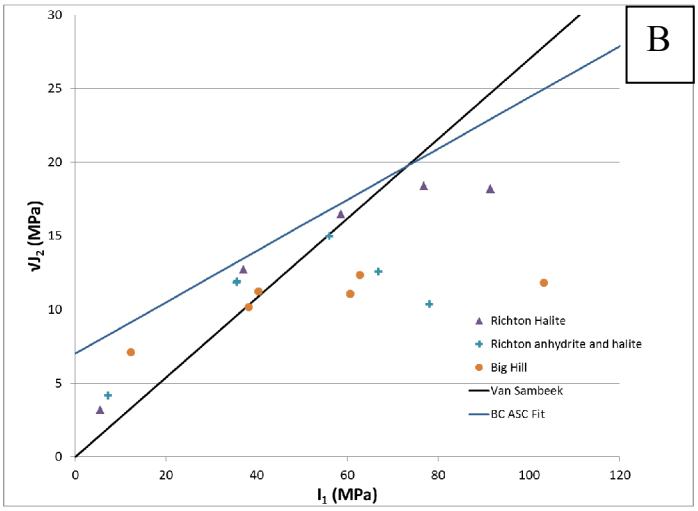

Fig. 4. Dilatant damage criterion for the salt tested. A) Data and fits determined by this study. B) Previous study data compared with the fits for this data.

Table 4. Tests performed under creep conditions, showing the stress difference, test duration, and values for the measured and calculated final axial strain rates. Tests were performed with 7.6 MPa confining pressure at 38° Celsius

Test I.D.	Stress Difference (MPa)	Test Duration (days)	Final Axial Strain Rate measured (s^{-1})	Final Axial Strain Rate calculated (s^{-1})
1	9.8	58	7.37E-10	6.52E-10
4	7.3	78	1.18E-10	1.89E-10
7	13.4	70	9.98E-10	2.31E-09
10	18.9	56	5.86E-09	9.18E-09
13	22.2	57	4.94E-09	1.80E-08
16	25.7	36	9.14E-09	3.22E-08
19	38.9	4	2.81E-07	1.75E-07

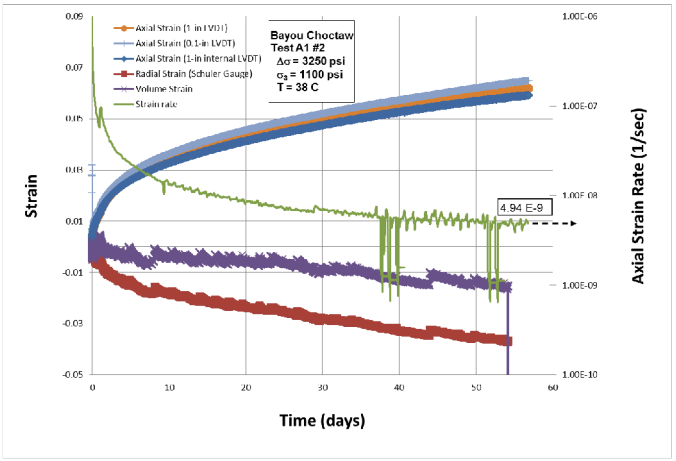

Fig. 5. Axial strain, radial strain and axial strain rate versus time for a typical creep test (Test #13).

A steady state strain rate analysis was performed for this rock salt. The small number of tests performed limits the creep expression to an estimate, as the effect of temperature and confining pressure were not investigated. A simplified steady-state only creep law (simplified due to the lack of temperature dependence) can be expressed by equation (4):

$$\dot{\varepsilon}_{ss} = A'\left(\frac{\Delta\sigma}{\mu}\right)^{n} \tag{4}$$

Where A' is a model parameter, $\Delta\sigma$ is the stress difference, μ is the elastic shear modulus, and n is a second model parameter. Based on the constant temperature assumption, the equation was linearized through a logarithmic transformation and fit with a straight line to determine a value for n=4.07. A value of n = 5 is typical of many salts [e.g., Munson et al, 1988]. The value of n determined from the linear transformation served as a constant for a nonlinear fitting process used to evaluate the model parameter A' in Equation 4 directly. Which was found to be A'=4.08x10^{10}. This leads to the steady state creep law determined for this salt as shown in equation 5.

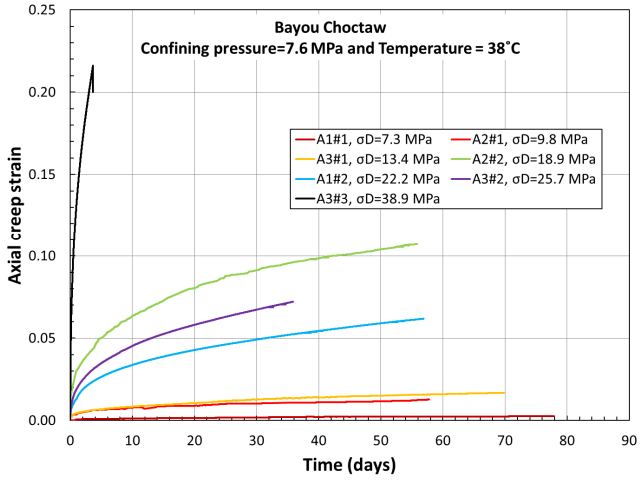

Fig. 6. Axial creep strain versus time for all creep tests.

$$\dot{\varepsilon}_{ss} = 4.08 \times 10^{10} \left(\frac{\Delta\sigma}{\mu} \right)^{4.07} \quad (5)$$

The values of n and A' were used in combination with equation 4 to predict the steady-state strain rates given in Table 4. These predictions or calculated steady-state rates are shown in Figure 7 and are in good agreement with the measured data.

In Figure 8 the creep expression estimate from this study to that of other rock salts is compared. In order to make a relative comparison, the BC creep data was plotted with the same slope as the other studies shown in Figure 8. To force the line to be parallel, the value of n from Equation 4 was set to 5 and A' was allowed to change; the steady state strain rates, shear modulus and stress difference from Equation 4 remained the same.

A value of A'=7.14x10^{13} was determined with the given value of n=5. Using n=5 is a common assumption in salt rock when an insufficient number of tests have been conducted to completely characterize the salt [10]. Figure 8 shows the BC rock salt creeps at an intermediate rate compared to other rock salts.

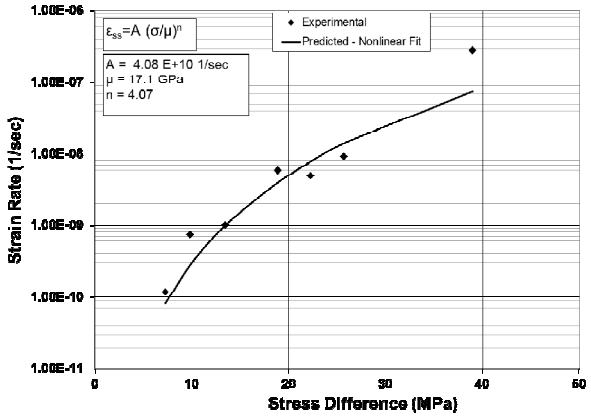

Fig. 7. Calculated and measured steady-state strain rates.

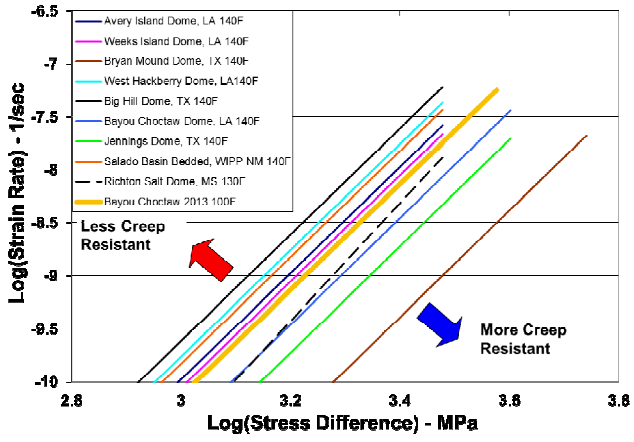

Fig. 8. Creep relation for Bayou Choctaw salt (thick orange line) compared with that of other Gulf Coast domal salts.

5. CONCLUSIONS

A laboratory testing program was used to examine the mechanical behavior of Bayou Choctaw salt for use in evaluation of a Strategic Petroleum Reserve Bayou Choctaw storage facility. Mechanical properties testing included: 1) ambient temperature quasi-static axisymmetric compression tests to evaluate dilational stress states and elastic properties; 2) ambient temperature quasi-static axisymmetric extension tests to evaluate dilational stress states and elastic properties; and 3) confined triaxial creep experiments to evaluate the time-dependent behavior of the salt at a constant confining pressure of 7.6 MPa at 38 °C.

It was found that the Young's modulus of the salt ranged from 27.2 to 58.7 GPa with an average of 44.4 GPa and generally increased with increasing mean stress. Poisson's ratio ranges from approximately 0.10-0.43 with an average of 0.30. The salt rock density was approximately 2.155 g/cc consistent with visual observational of near pure halite content. A dilatational strength criteria was determined for this work defined by equation 3 for the extension tests, and equation 4 for the compression tests.

A steady-state-only creep model has been developed. The creep model suggests that BC rock salt has an intermediate creep resistance when compared to other rock salts.

6. ACKNOWLEDGEMENTS

Sandia National Laboratories is a multi-program laboratory managed and operated by Sandia Corporation, a wholly owned subsidiary of Lockheed Martin Corporation, for the U.S. Department of Energy's National Nuclear Security Administration under contract DE-AC04-94AL85000. SAND2015-XXXX

REFERENCES

1. Park, B-Y., B.L. Ehgartner, and M.Y. Lee. 2006, Three Dimensional Simulation for Bayou Choctaw Strategic Petroleum Reserve (SPR), SAND2006-7589, Sandia National Laboratories, Albuquerque, New Mexico.

2. DeVries, K.L., K.D. Mellegard, and G.D. Callahan. 2003. Laboratory Testing in Support of a Bedded Salt Failure Criterion, In *Proceedings of the Solution Mining Research Institute Fall Meeting*, Chester UK.

3. Munson, D.E., A.F. Fossum, and P.E. Senseny. 1988. Advances in Resolution of Discrepancies Between Predicted and Measured In Situ WIPP Room Closures, *SAND88-2948*, Sandia National Laboratories, Albuquerque, NM.

4. ASTM D4543, 1995. Standard Practice for Preparing Rock Core Specimens and Determining Dimensional

and Shape Tolerances, American Society for Testing and Materials.

5. Labuz, J.F., and J.M. Bridell. 1993, Reducing frictional constraint in compression testing through lubrication, *Int. J. Rock Mech. Min. Sci.* 451-455.

6. Mellegard, K. D. and T. W. Pfeifle, 1994. Laboratory Testing of Dome Salt from Weeks Island, Louisiana in Support of the Strategic Petroleum Reserve (SPR) Project, *RSI-0552*, RE/SPEC Inc., Rapid City, SD.

7. Lee, M.Y., B.L. Ehgartner, and D.R. Bronowski. 2004. Laboratory Evaluation of Damage Criteria and Permeability of Big Hill Salt, *SAND2004-6004*, Sandia National Laboratories, Albuquerque, NM 87185.

8. Broome, S.T., S.J. Bauer, D. Dunn, J.H. Hofer, and D.R. Bronowski. 2009. Geomechanical Testing of MRIG-9 Core for the Potential SPR Siting at the Richton Salt Dome, *SAND2009-0852*, Sandia National Laboratories, Albuquerque, New Mexico.

9. Van Sambeek, L. L, Ratigan, J. L., and F. D. Hansen, 1993. Dilatancy of Rock Salt in Laboratory Tests, Int. J. Rock Mech. Min. Sci. & Geomech. Abstr. 735-738.

10. Fossum, A.F., and J.T. Fredrich. 2002. Salt Mechanics Primer for Near-Salt and Sub Salt Deepwater Gulf of Mexico Field Developments, *SAND2002-2063*, Sandia National Laboratories, Albuquerque, New Mexico.